ISSN: 2447-3359

REVISTA DE GEOCIÊNCIAS DO NORDESTE

Northeast Geosciences Journal

v. 11, nº 1 (2025)

https://doi.org/10.21680/2447-3359.2025v11n1ID39415

Granulometric characterization of the alluvial-colluvial deposits in microbasins of the Copiapó river – Atacama region (Chile).

Caracterização granulométrica dos depósitos alúvio-coluviais de microbacias do rio Copiapó – região de Atacama (Chile).

Keyla Manuela Alencar da Silva Alves[1]; Drielly Fonseca[2]; Marcelo Lagos[3]; Jaime Carrasco Barra[4]

[1] Universidad Tecnológica Metropolitana, Facultad de Ingeniería, Departamento de Industria, Escuela de Geomensura. Santiago, Chile. E-mail: keyla.dasilva@utem.cl
ORCID: http://orcid.org/0000-0001-7635-2430

[2] Universidad Tecnológica Metropolitana, Facultad de Ingeniería, Departamento de Industria, Escuela de Geomensura. Santiago, Chile. E-mail: dfonseca@utem.cl
ORCID: https://orcid.org/0000-0002-1374-8697

[3] Pontifícia Univesidad Católica de Chile, Facultad de Historia, Geografía y Ciencia Política, Instituto de Geografía, Santiago, Chile. E-mail: mlagoslo@uc.cl
ORCID: https://orcid.org/0009-0002-8320-5855

[4] Universidad Tecnológica Metropolitana, Facultad de Ingeniería, Departamento de Industria, Escuela de Industria. Santiago, Chile. E-mail: jcarrascob@utem.cl
ORCID: https://orcid.org/0000-0003-4123-4228

Abstract: This study aims to characterize the grain size distribution of sediments in alluvial-colluvial deposits within the Copiapó River basin, Chile, to provide detailed information on their composition and enhance the understanding of debris flow behavior. Debris flows are mass-wasting events triggered by intense and localized rainfall, commonly occurring in the arid zones of the Coastal Range and the Andes. These flows are defined by their high density and a composition largely made up of gravel mixed with water, giving them non-Newtonian and viscoplastic fluid properties that enable the transport of large volumes of material. Grain size analysis revealed that the studied microcatchments contain sediments with low cohesion and high susceptibility to erosion, predominantly composed of angular and non-cohesive gravel and sand particles. These characteristics facilitate the initiation and mobilization of debris flows on steep slopes, which is typical of arid regions with high erosive energy. This research contributes to clarifying the relationship between sediment composition and debris flow dynamics, offering key granulometric data for the characterization of materials transported during mass movement events.

Keywords: Granulometric composition; Debris flows; Copiapó river basin.

Resumo: Este estudo tem como foco caracterizar a granulometria dos sedimentos presentes em depósitos aluvio-coluviais da bacia do rio Copiapó, no Chile, com o objetivo de gerar informações detalhadas sobre sua composição e contribuir para a compreensão do comportamento dos fluxos de detritos (aluviais). Esses fluxos correspondem a eventos de movimento em massa, desencadeados por precipitações intensas e concentradas, sendo frequentes nas zonas áridas da Cordilheira da Costa e da Cordilheira dos Andes. Caracterizam-se por sua alta densidade e por uma mistura de cascalhos e água que lhes confere propriedades de fluido não-newtoniano e viscoplástico, permitindo-lhes mobilizar grandes volumes de material. Os resultados da análise granulométrica indicam que as microbacias avaliadas contêm sedimentos com baixa coesão e alta suscetibilidade à erosão, predominando partículas angulosas e não coesas de cascalhos e areias. Essas características favorecem a geração e o transporte de fluxos de detritos em encostas íngremes, típicas de regiões áridas com alta energia erosiva. O estudo contribui para estabelecer vínculos entre a composição dos sedimentos e a dinâmica dos fluxos, fornecendo dados relevantes para a caracterização do material transportado em eventos de movimento em massa.

Palavras-chave: Composição granulométrica; Fluxos de detritos; Bacia do rio Copiapó.

Received: 12/03/2025; Accepted: 05/05/2025; Published: 13/06/2025.

1. Introduction

The grain-size composition of sediments is a critical factor when classifying flow types. Debris flows are typically composed of a high percentage of coarse-grained material mixed with a smaller but dynamically significant proportion of fine particles, primarily clays. These flows occur at variable velocities, depending on factors such as water content, local slope, and other frictional parameters (Jaapar et al., 2023; Zainol & Awahab, 2018; Elmes, 2016).

In this context, the granulometry of sediments deposited in channels, riverbeds, and ravines emerges as a key parameter for determining flow type, energy, and velocity. Sediments found in arid environments—such as those examined in this study—tend to be heterogeneous in terms of both particle size and mineral composition (Gonçalves et al., 2021; Sivak & Volkova, 2020; Antoni et al., 2019; Pranoto & Subari, 2019). The particle size distribution, ranging from clays to gravels, plays an essential role in defining the rheological and transport properties of debris flows. Fine and cohesive particles increase the viscosity of the suspension, thereby inhibiting rapid sedimentation and promoting debris flow formation (Gutiérrez et al., 2018; Haas & Woerkom, 2016; Bin & Ming, 2014).

More than 80% of the solid mass in debris flows typically consists of particles larger than 2 mm, with the remaining 20% composed of particles smaller than 2 mm (on average). Debris flows are characterized by water-saturated material with a high concentration of solids that behaves mechanically as a non-Newtonian fluid. As the solid content increases and the density of the mixture exceeds that of water, its resistance to deformation also increases, making the relationship between shear stress and deformation rate non-linear. In general, debris flows exhibit high density (60–70% solids by weight), with 20–80% of the particles exceeding 2 mm in size. These flows have a high transport capacity and can carry large boulders and objects such as vehicles, houses, and infrastructure (Hu et al., 2017; Pellegrino & Schippa, 2017; Wu et al., 2015).

Among the key factors influencing the mechanical behavior of debris flows are the grain-size distribution of the matrix and the volumetric concentration of fine sediments. The percentage of fine particles (<100–200 μm) in the mixture significantly affects the mechanical behavior and velocity of the flow (Wu et al., 2021; Blasio, 2011). Debris flows generally behave as viscoplastic fluids, characterized by a minimum yield stress, above which the material begins to move. This is due to the interplay between interstitial fluid and particle interactions.

If the source matrix contains more than 10% fine particles, the interstitial fluid lubricates the sediment particles. For such small-diameter grains, viscosity dominates the fluid mechanics. Conversely, if the matrix contains less than 10% of fine sediments, flow dynamics are governed by direct contact between gravel particles, and inertial forces prevail (Llorente et al., 2023; López et al., 2021; Moreno, 2014).

Empirical studies and numerical modeling have provided a robust foundation for understanding how variations in particle size distribution influence debris flow behavior (Iverson & George, 2023). Moreover, sediment susceptibility to erosion and mobilization—combined with local hydroclimatic and topographic conditions—contributes to the frequency and magnitude of these events (Ouyang et al., 2019; Hürlimann et al., 2019).

This study aims to characterize the grain-size distribution of alluvial-colluvial deposits located in sediment source zones within six micro-watersheds of the Copiapó River basin, Atacama Region, northern Chile.

2. Methodology

2.1 Study Area

The micro-watersheds selected for this study are in the lower sub-basin of the Copiapó River, downstream from the confluence of the Copiapó River and the Paipote Ravine (Figure 1a). The analyzed micro-watersheds are situated along the hillslopes that border the northern edge of the city of Copiapó (Figure 1b).

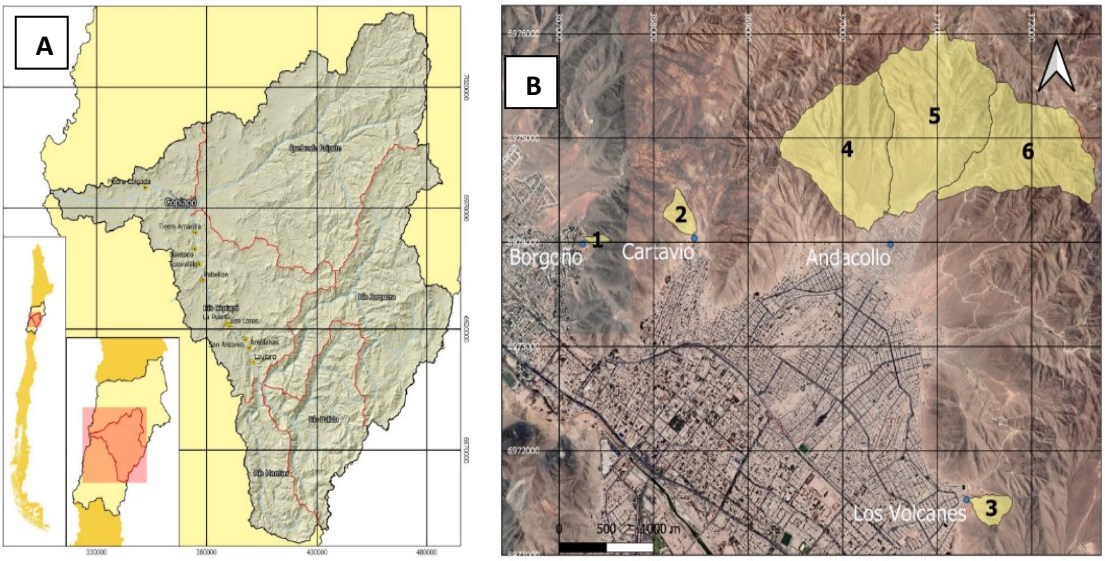

Micro-watershed	Settlement	Total Area (km²)	Average Basin Slope (m/m)	Minimum Elevation (m a.s.l.)	Maximum Elevation (m a.s.l.)	Channel Length (m)
1	Borgoño	0.019	0.28	408.0	531.1	250.7
2	Cartavio	0.087	0.33	484.7	690.8	478.0
3	Los Volcanes	0.094	0.26	474.4	630.4	573.8
4	Andacollo (left)	1.142	0.29	535.4	1012.4	1630.0
5	Andacollo (center)	1.473	0.28	556.6	1007.0	2291.0
6	Andacollo (right)	1.007	0.34	606.8	984.1	2005.5

Figure 1a and 1b – Characteristics of the selected micro-watersheds in the lower sub-basin of the Copiapó River. Source: Authors (2024).

In the Copiapó River basin, the channels flow over geological strata composed of fluvio-alluvial deposits, such as gravels, sands, and silts, originating from both modern rivers and their associated terraces and floodplains (DGA – CONAMA, 2009, as cited in Araneda, 2016). According to the Copiapó Geological Map (Arévalo, 2005) at a 1:100.000 scale, the basin is predominantly composed of Mesozoic rocks, including Cretaceous intrusive rocks, sedimentary units, and volcanic formations (Figure 2). These are overlain by unconsolidated deposits ranging from the Miocene to the present day (Larrondo, 2017).

The micro-watersheds selected for this study are in urbanized areas, with informal settlements (campamentos) established on ancient alluvial and colluvial deposits (MsPliac), as well as on inactive alluvial deposits (PIHa). Furthermore, in micro-watersheds 4, 5, and 6 (Andacollo sector), part of the area lies within the Punta del Cobre Formation (JKpc), a geological unit consisting of a volcanic-sedimentary sequence.

The Punta del Cobre Formation is present on both flanks of the Copiapó River valley and the Paipote ravine. Its lithology is heavily altered, comprising volcanic and clastic sections. Ancient alluvial and colluvial deposits (MsPliac) are found in micro-watershed 1 (Borgoño sector), micro-watershed 2 (Cartavio sector), and others, characterized by features such as alluvial fans and colluvial accumulations. Inactive alluvial deposits (PIHa) are observed in areas such as the southern part of micro-watershed 1 and portions of micro-watersheds 3 (Los Volcanes sector), 4, 5, and 6, where the sediments appear consolidated and show no evidence of recent activity.

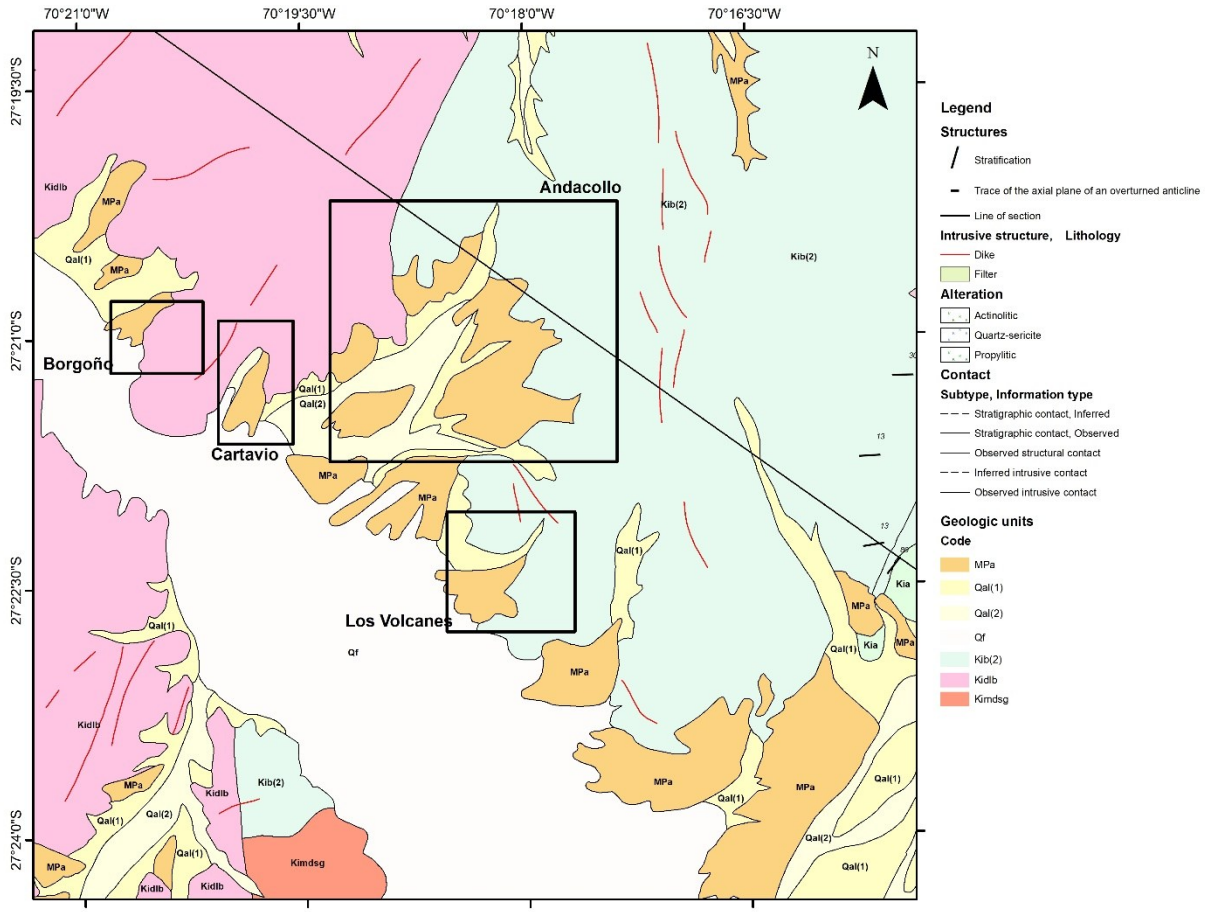

Figure 2 – Geological characterization of the micro-watersheds in the lower sub-basin of the Copiapó River. Source: Arévalo (2005), modified by the authors (2025).

The geomorphology of the Copiapó River basin is characterized by an irregular topography with transverse valleys and mountainous ranges. The main physiographic elements include the Andes Mountains, Transverse Valleys, Coastal Range, and Coastal Plains (Figure 3). The urban area of the Copiapó municipality is situated on an alluvial plain at the confluence of the Paipote Ravine and the Copiapó River, surrounded by hills of varying elevations. Episodes of intense rainfall activate the transverse ravines, transporting sediments toward the river and potentially causing overflows (Izquierdo et al., 2024; Gonzales et al., 2023). The valley soils consist of fluvial sediments, with youthful landforms in the upper and middle sections, and a peneplain with gentler slopes in the lower reaches (Bäuerle et al., 2010; Correa et al., 2009).

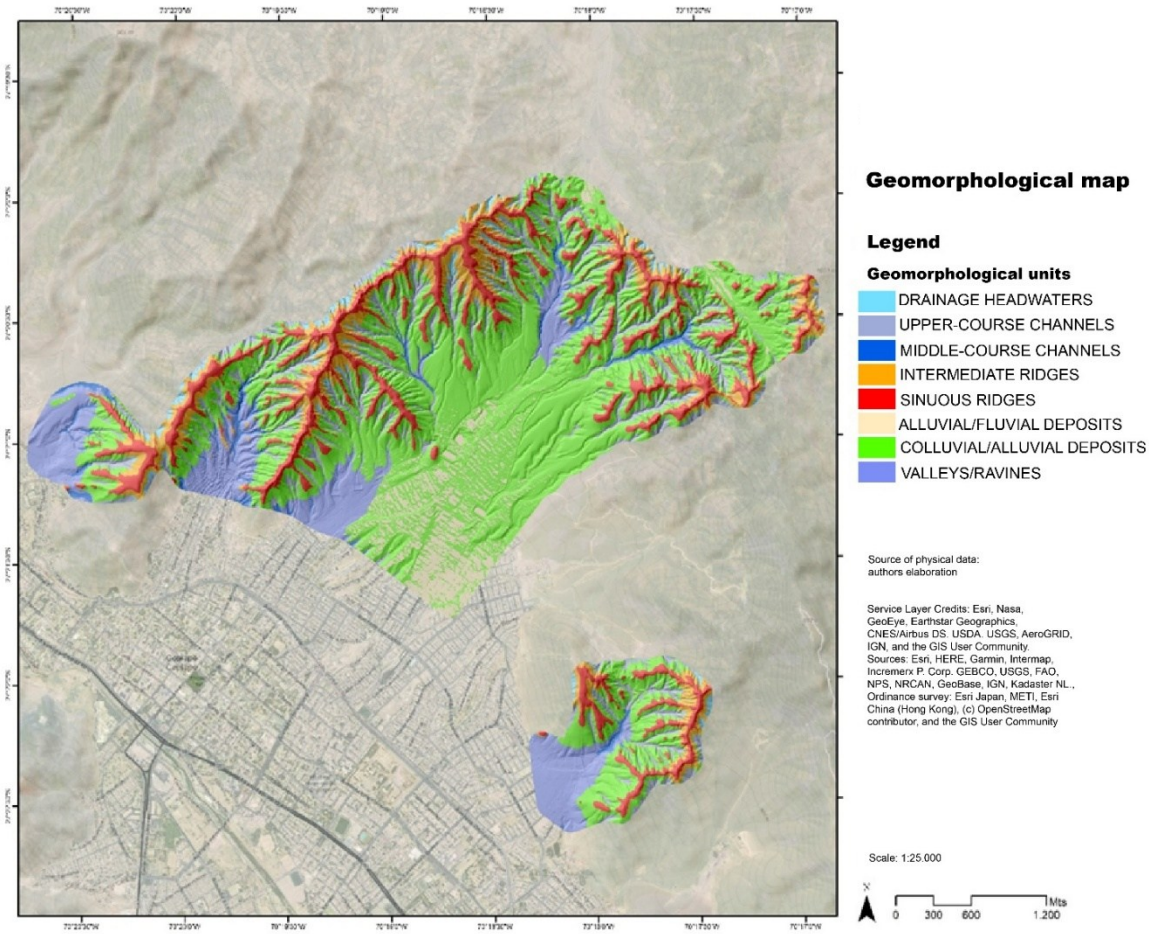

Figure 3 – Geomorphological characterization of the selected micro-watersheds in the lower sub-basin of the Copiapó River.
Source: Authors (2025).

2.2 Field Data Collection

Sampling sites were selected based on their accessibility and geological representativeness within the studied micro-watersheds, with priority given to areas containing well-preserved deposits that allowed for the analysis of sedimentary sequences and recent geomorphological processes (Martínez & Fernández, 2023).

A total of 13 samples were collected from deposits located in the upper, middle, and lower sections of the ravines, as well as from alluvial fans (Figure 4). In alluvial deposits with intact stratification, a systematic sampling protocol was followed to collect material from each individual layer, ensuring proper representation of the physical characteristics throughout the sedimentary profile. This approach enables interpretation of the fluvio-alluvial dynamics over time (García & Ruiz, 2022; López et al., 2021; Smith & Jones, 2020; Thompson et al., 2019).

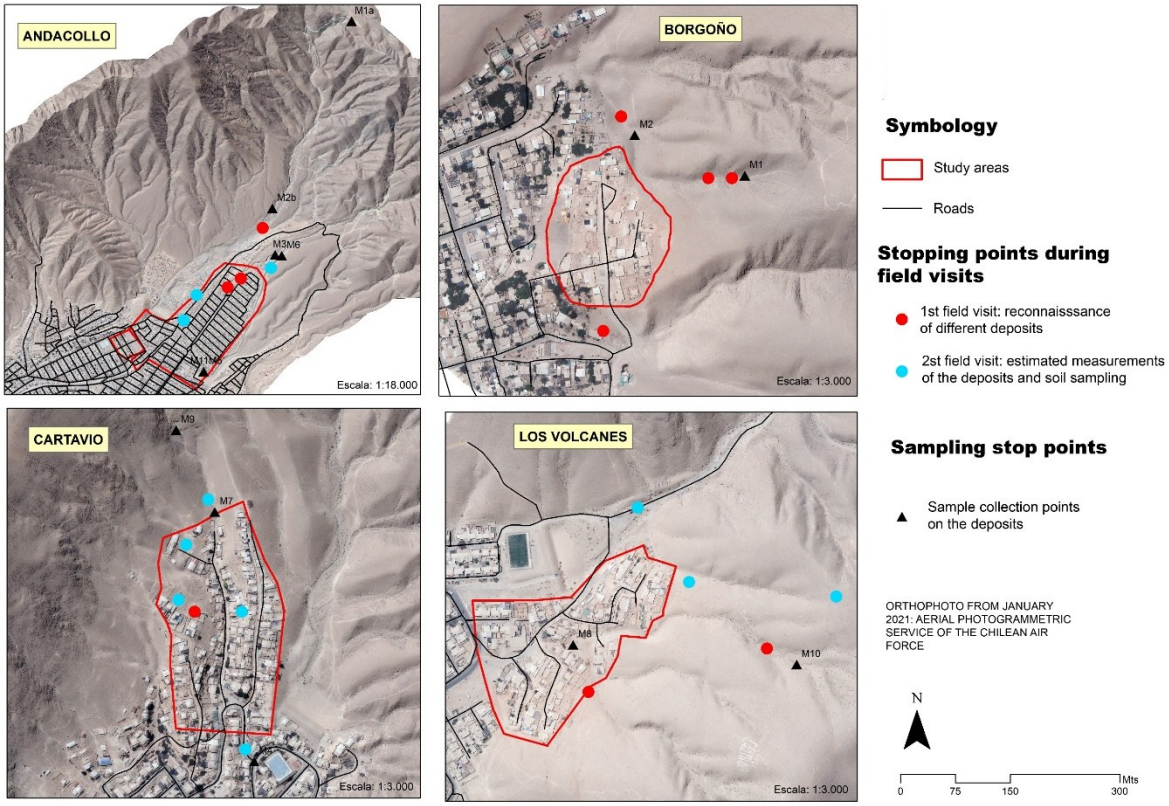

Figure 4 – Sampling points and field visits in the selected micro-watersheds.
Source: Authors (2025).

2.3 Laboratory Procedures

2.3.1 Mechanical Sieving Method

Grain-size analysis by mechanical sieving is a standardized procedure used to determine the percentage of mass retained on each sieve relative to the total mass of the original sample. The relationship between the weight of sediments retained and those passing through each selected sieve allows for the determination of the particle size distribution model (Cesta et al., 2016; Klein et al., 2013; Arche, 2010). The calibration parameters for the mechanical sieve shaker were set according to ISO 18400-104, *Soil quality — Sampling — Part 104: Strategies*. The selection of sieve apertures representative for quantifying sand and silt concentrations followed the ASTM D422-63 standard.

Additionally, colorimetric characterization of the samples was performed using the Munsell soil color chart, and clay content was determined using the Stokes' sedimentation method. Sample preparation followed the *Recommended Methods of Soil Analysis for Chile* (Sadzawka et al., 2006). All pre- and post-sieving and pipetting procedures were applied to the 13 collected samples. These procedures are illustrated in Figure 5.

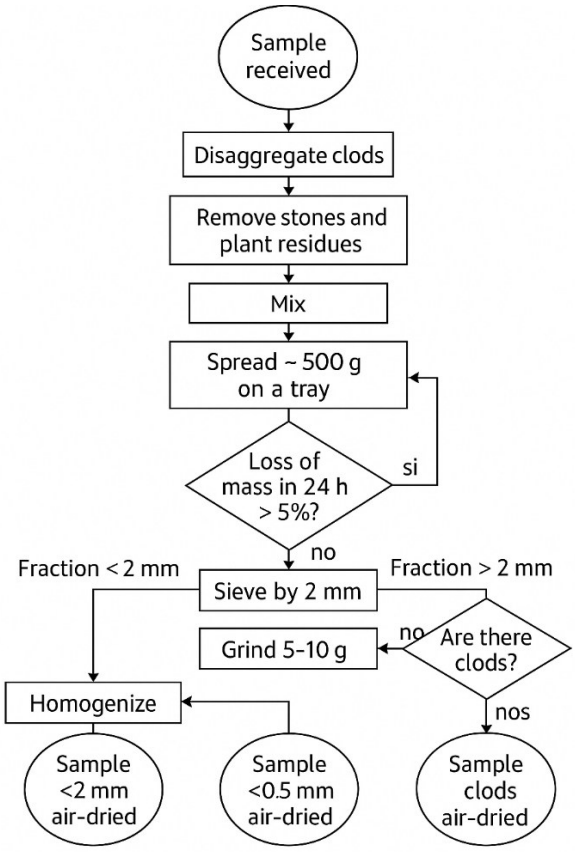

Figure 5 – Diagram of sample preparation procedures prior to sieving. Source: Sadzawka et al. (2006).

To carry out the sieving process, the sieves were arranged in descending order with the following mesh sizes: 2 mm, 850 µm, 250 µm, 90 µm, 63 µm, 53 µm, 45 µm, and 38 µm. Each sample was initially placed on the uppermost sieve. The procedure was conducted over a 10-minute period using an analytical sieve shaker, operating at an amplitude of 3.00 with no intermediate pauses.

2.3.2 Stokes' Method

The pipette method based on Stokes' law is employed when sediments contain fine particles (fine silts and clays) that cannot be accurately measured by mechanical sieving. The method relies on Stokes' Law (Stokes, 1851), which states that a particle of a given diameter and density, when deposited into a 1-liter water mixture with 10 grams of sodium hexametaphosphate, will settle at a velocity determined by its volume, gravitational acceleration, the viscosity of the fluid, and the density contrast between the particle and the fluid (Leyva et al., 2016). For particles smaller than 0.1 mm (finer than very fine sand), the resistance exerted by the fluid is proportional to the product of the particle's diameter, its velocity, and the fluid's viscosity (Filgueira et al., 2006) (Figure 6).

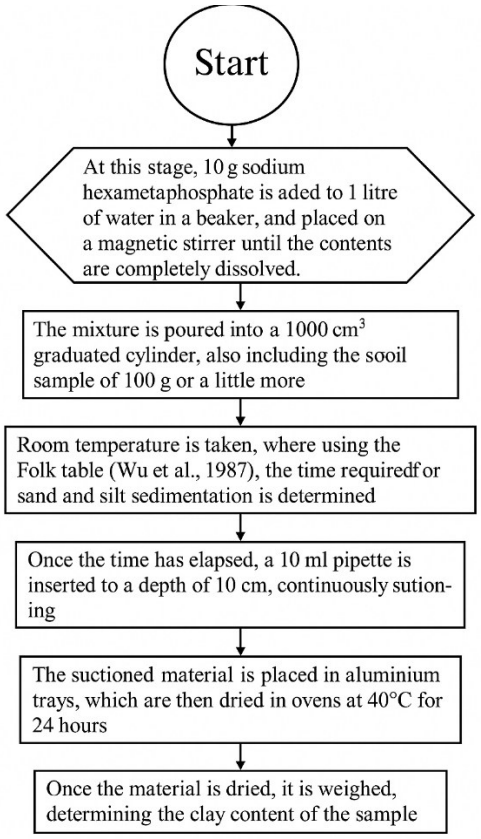

Figure 6 – Diagram of the procedures for applying Stokes' method.
Source: Authors (2024).

2.3.3 Statistical Analysis Method

Statistical calculations were applied to obtain the mass balance, assess the precision of the process, and quantify measurement error, with the aim of identifying and analyzing potential causes of deviations in the obtained results. These calculations were performed using the following equations:

1. Retained Weight Fraction

$$fx_i = m_i \sum_{i=1}^{n} m_i$$

mi it is the weight retained on each sieve

2. Cumulative Fines Fraction

$$F(x_i = \sum_{i=1}^{n} f(x_i)$$

3. Cumulative Retained Fraction

$$R(x_i) = \sum_{i=1}^{n} f\,(x_{i)} = 1 - F(x_i)$$

4. Percentage of Error

$$\%\ \text{Error} = \frac{\text{initial weight} - \text{final weight}}{\text{initial weight}}\ x\ 100$$

The particle size distribution was examined through grain-size distribution curves, which represent the cumulative proportion of each fraction as a function of particle size. Statistical analyses of texture, sorting, skewness, and kurtosis (Table 1) were performed using grain-size data processed with the Sysgran software.

Table 1 – Interpretative values used in the statistical analysis of the samples.

Sorting $\sigma_\phi = \sqrt{\frac{\sum f(m_\phi - x_\phi)^2}{100}}$		Skewness $sk_\phi = \frac{\sum f(m_\phi - x_\phi)^3}{100^3_\phi}$		Kurtosis $K_\phi = \frac{\sum f(m_\phi - x_\phi)^4}{100^4_\phi}$	
Very well sorted	<0.35	Very negatively skewed	<-1.3	Very platykurtic	<1.70
Well sorted	0.35 – 0.5	Negatively skewed	-1.3 - -0.43	Platykurtic	1.70 – 2.55
Moderately well sorted	0.5 – 1.0	Approximately symmetric	-0.43 - 0.43	Mesokurtic	2.55 – 3.7
Poorly sorted	1.0 – 2.0	Positively skewed	0.43 – 1.3	Leptokurtic	3.7 – 7.4
Very poorly sorted	2.0 – 4.0	Very positively skewed	>1.3	Very leptokurtic	7.4 - 15
Extremely poorly sorted	>4			Extremely leptokurtic	>15
f = cumulative weight percentage retained on each sieve m= median of the particle diameter range in phi (ϕ)					

Source: Camargo (2006).

3. Results and Discussion

A total of 13 samples were collected from alluvial and colluvial deposits across different micro-watersheds within the Copiapó River basin, including the sectors of Borgoño (micro-watershed 1), Cartavio (micro-watershed 2), Los Volcanes (micro-watershed 3), and Andacollo (micro-watershed 5). These deposits were selected to analyze grain size distribution, sediment texture, and statistical properties, following the nomenclature and order described in the methodology (Figure 4). No samples were collected from micro-watersheds 4 and 6 in the Andacollo sector due to the instability of unconsolidated deposits and access limitations.

3.1 Micro-watershed 1 (Borgoño Sector)

Two sediment samples were collected from the main ravine in this micro-watershed, one upstream (M1) and one downstream (M2), to assess textural variability. The sediments exhibit a coarse sand texture with angular grains, predominantly of alluvial-colluvial origin, attributed to weathering, erosion, and transport from surrounding areas. Structurally, the deposits show well-developed coarse polyhedral aggregates, with moderate plasticity and medium

friability under moist conditions; when dry, they become compacted and resistant to crumbling. Scattered ferruginous nodules were observed, likely related to iron segregation processes.

Grain-size analysis revealed a high concentration of coarse particles (gravel and sand), exceeding 90% in both samples. In M1, the composition was 13.51% gravel, 83.43% sand, 2.73% silt, and 0.33% clay, while in M2 it was 13.25% gravel, 84.19% sand, 2.28% silt, and 0.28% clay. Fine sediments (<200 micrometers) accounted for 1.53% in M1 and 1.28% in M2, consistent with typical alluvial environments (Moreno, 2014).

In M1, the flow is more turbulent due to steeper slopes and a lower accumulation of fine particles, with a high proportion of coarse sand (83.43%), indicating sufficient energy to transport large particles, but not a significant amount of gravel. In contrast, M2 shows a more stable and less turbulent flow, with a slight decrease in gravel and a higher concentration of sand (84.19%). The downstream reduction in skewness and kurtosis reflects slower and more uniform depositional conditions. The grain-size characteristics and overall analysis suggest a transitional to turbulent flow regime in the Borgoño sector. The high proportion of coarse sand and the low compaction of sediments indicate an environment with active, though not extreme, sediment transport (Figure 7).

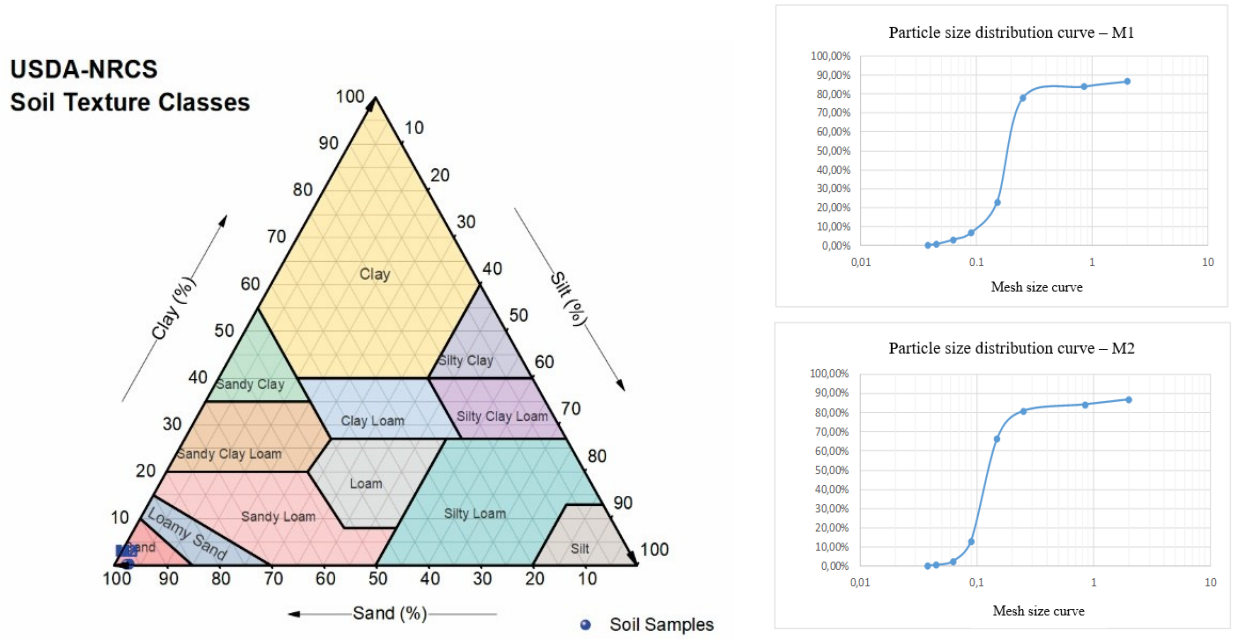

Figure 7 – Textural analysis results and grain-size distribution curves for samples M1 and M2 from micro-watershed 1, Borgoño sector.
Source: Authors (2024).

A minimal weight loss was observed in the samples: 2% in M1 and 1% in M2, indicating low compaction and limited mechanical wear, possibly due to less intense flow conditions. The uniform sampling depth (50 cm) and consistent lithology suggest a common origin of the sediments, likely transported, and deposited by flows originating from the surrounding mountains. The Munsell color analysis (10 YR 6/3) revealed moderate oxidation and the presence of iron minerals, with similar oxidation conditions at both sampling points.

The grain-size properties indicated a moderately well-sorted mixture of grain sizes (σ_ϕ: 1.26 in M1, 1.34 in M2), with a predominance of coarse particles (α_ϕ: –0.33 in M1, –0.64 in M2) and high kurtosis values (K_ϕ: 1.92 in M1, 1.41 in M2), which are indicative of rapid and relatively uniform deposition processes (Hetz et al., 2013; Antinao & McDonald, 2013).

Table 2 – Sysgran analysis results for samples M1 and M2 – micro-watershed 1, Borgoño sector.

Site	Sample	UTM East	UTM South	Depth (M/Cm)	Initial Weight (g)	Final Weight (g)	Error %	Munsell Color	Sorting (Σ_Φ)	Skewness (A_Φ)	Kurtosis (K_Φ)
Upstream	M1	367415	6974046	50cm	1021,01	1001,01	2%	10 YR 6/3 (light yellowish brown)	1.26	-0.33	1.92
Downstream	M2	367285	6974094	50cm	1019,25	1005,25	1%	10 YR 6/3 (light yellowish brown.)	1.34	-0.64	1.41

Source: Authors (2024).

3.2 Micro-watershed 2 (Cartavio Sector)

Three samples were collected from this micro-watershed—two upstream (M7 and M9) and one downstream (M4)—from alluvial-colluvial deposits. Grain-size analyses revealed significant variations in composition, reflecting different transport and depositional conditions.

Sample M4, collected downstream, showed a higher concentration of gravel (64.19%), sand (28.08%), silt (6%), and clay (1.73%), with predominantly angular grains and low cohesion. These characteristics suggest active transport processes associated with recent mass-wasting events. Its well-developed coarse polyhedral structure, moderate plasticity, and dry hardness further support this interpretation. The concentration of fine sediments was 3.86%, within the typical range for alluvial environments in arid zones (Moreno, 2014).

In contrast, samples M7 (33.74% gravel, 58.39% sand, 5.48% silt, and 2.40% clay) and M9 (8.42% gravel, 88.26% sand, 3.01% silt, and 0.30% clay), collected upstream, reflect lower-energy flows compared to M4. In M7, transitional flow conditions transported intermediate materials, as indicated by a moderately developed fine polyhedral structure and a fine sediment content of 3.94%. M9, with 88.26% sand and only 8.42% gravel, suggests a more stable and uniform flow, likely due to lower slope gradients or increased distance from coarse sediment sources, with a fine sediment concentration of 1.67%. The higher proportion of coarse particles in M4 indicates turbulent flows and rapid deposition, whereas M7 and M9 reflect more stable and homogeneous flow regimes (Figure 8).

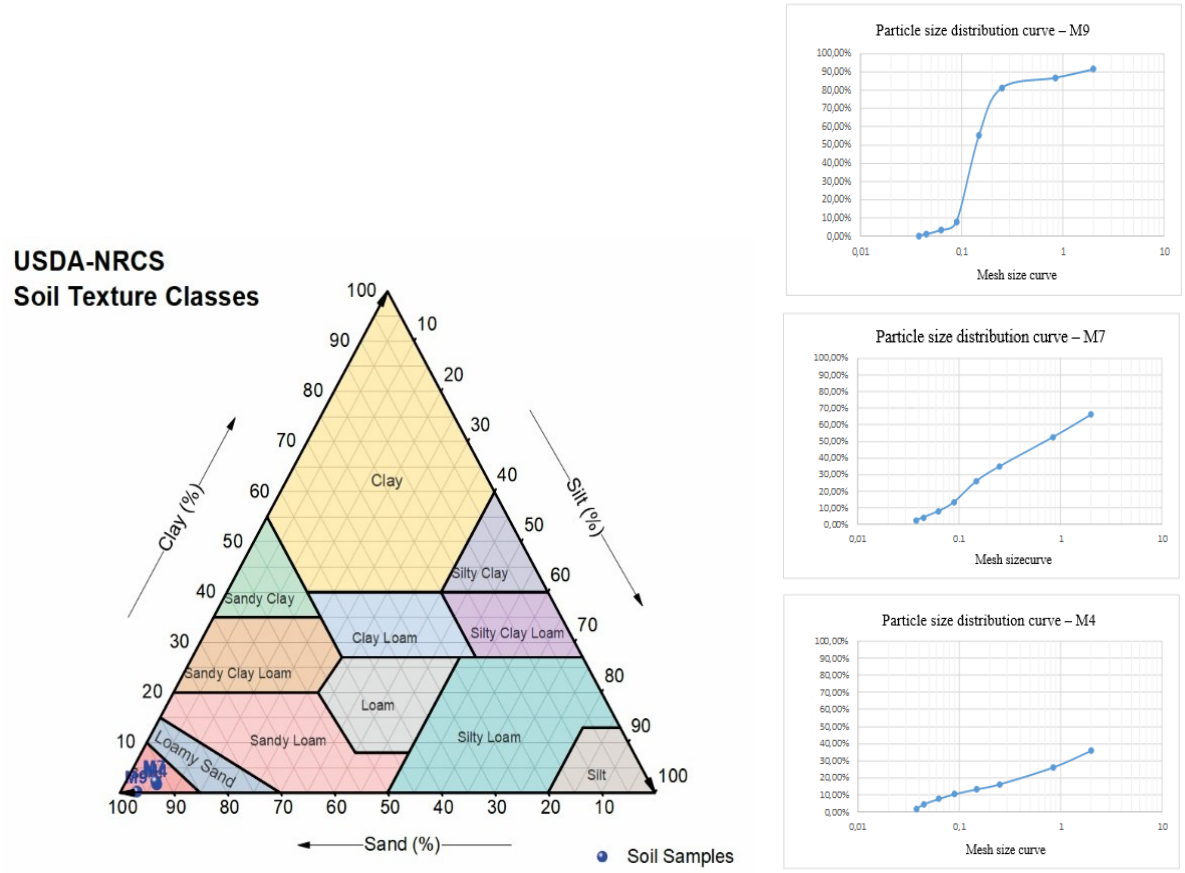

Figure 8 – Textural analysis results and grain-size distribution curves for samples M4, M7, and M9 from micro-watershed 2, Cartavio sector.
Source: Authors (2024).

The samples showed variations in weight loss, ranging from 0% in M9 (1 m depth) to 3% in M4 (6 m depth), indicating differences in compaction and moisture content. Sampling depths varied from 90 cm to 6 m, suggesting different levels of alluvial deposition and colluvial processes, associated with a common sediment source (Yu et al., 2016; Sohn et al., 2007; Kiersch, 1996). Color analysis revealed significant differences among the samples—10 YR 5/4 in M4, 7.5 YR 5/4 in M7, and 10 YR 6/3 in M9—reflecting variations in oxidation and redox conditions during deposition (Bourquin et al., 2009).

Grain-size properties also revealed variability in transport and depositional processes. Sorting ranged from moderately well sorted (σ_ϕ: 1.24 in M9) to poorly sorted (σ_ϕ: 1.71 in M7). Skewness varied from negative values (–0.51 in M4, indicating a dominance of coarse particles) to positive values (1.38 in M9, indicating a predominance of fine particles), while kurtosis ranged from 0.5 in M7 (a flat distribution) to 1.39 in M9 (a more peaked distribution) (Liu et al., 2014; Summa-Nelson & Rittenour, 2012; Nichols & Fisher, 2007; Griffiths et al., 2006; Rommens et al., 2006).

Table 3 – Sysgran analysis results for samples M4, M7, and M9 – micro-watershed 2, Cartavio sector.

Site	Sample	UTM East	UTM South	Depth (M/Cm)	Initial Weight (g)	Final Weight (g)	Error %	Munsell Color	Sorting (Σ_Φ)	Skewness (A_Φ)	Kurtosis (K_Φ)
Middle course	M4	370885	6974649	6m	941,56	911,44	3%	10 YR 5/4 (moderate yellowish brown)	1.27	-0.51	1.23
Downstream	M7	368410	6974183	90cm	1056,3	1040,3	2%	7.5 YR 5/4 (moderate (reddish) brown)	1.71	0.31	0.5

Upstream	M9	368356	6974298	1m	1048,09	1044,09	0%	10 YR 6/3 (light yellowish brown)	1.24	1.38	1.39

Source: Authors (2024).

3.3 Micro-watershed 3 (Los Volcanes Sector)

Two samples were collected from micro-watershed 3 in the Los Volcanes sector: M8, located downstream (33.27% gravel, 61.70% sand, 4.34% silt, 0.69% clay), and M10, located upstream (22.40% gravel, 69.75% sand, 6.91% silt, 0.94% clay). Both samples come from alluvial-colluvial deposits, and their grain-size and textural characteristics reflect sediment transport and depositional dynamics.

Coarse sand predominates in both samples, with angular, loose, and relatively uniform grains, indicating a moderate- to high-energy depositional environment. Sample M8 exhibits a moderately developed fine polyhedral structure, reddish-yellow stains associated with oxidation and weathering, and physical properties including low plasticity and dry hardness. In contrast, M10 has a more compact coarse polyhedral structure, suggesting greater consolidation under more stable depositional conditions. Fine sediment concentrations (<200 micrometers) were 2.51% in M8 and 3.92% in M10, typical of alluvial environments in arid regions (Moreno, 2014).

Downstream sample M8 contains a higher proportion of gravel (33.27%) and less sand (61.70%), indicating a more active and turbulent flow. Conversely, upstream sample M10 has a higher sand content (69.75%) and lower gravel content (22.40%), suggesting a less intense flow, though still capable of transporting coarse particles. Both samples show negative skewness (−0.25 in M8 and −0.55 in M10), typical of coarse sediments in high-energy settings, and low kurtosis (0.40 in M8 and 0.48 in M10), indicating a flat and uniform grain-size distribution.

The stability in moisture content and minimal weight loss (0% in both samples) suggests weakly erosive flows with recent or moderately stable deposition. The consistent sampling depth (92–98 cm) and similar lithological characteristics indicate a common sediment origin, likely transported by intermittent flows in arid climates. Color differences between the samples reflect local variations in oxidation and weathering, influenced by redox conditions (Figure 9).

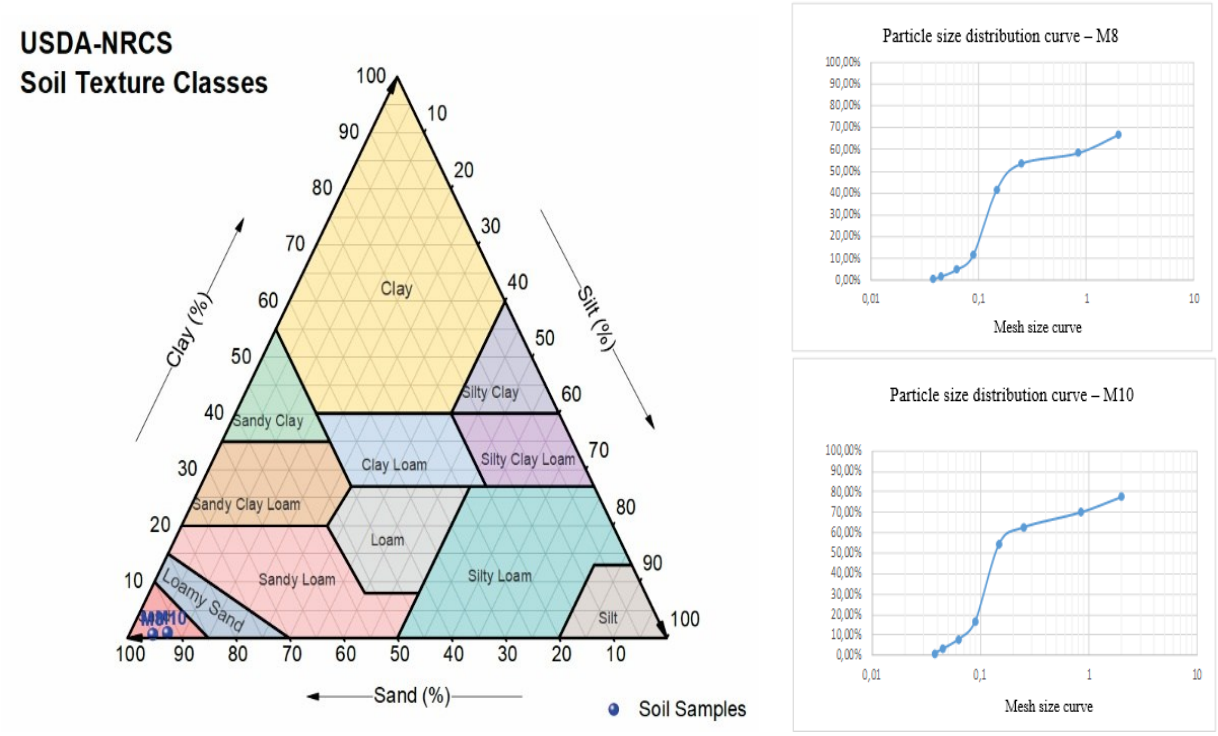

Figure 9 – Textural analysis results and grain-size distribution curves for samples M8 and M10 from micro-watershed 3, Los Volcanes sector.
Source: Authors (2024).

Samples M8 and M10 exhibited no weight loss (0%), indicating low compaction and minimal mechanical wear, likely due to less intense flow conditions. The uniform moisture content suggests stable humidity levels at the time of sampling (Regmi & Rasmussen, 2018; Löhrer et al., 2013). The consistent sampling depths, approximately 1 meter, reflect shallow, homogeneous alluvial sediments characteristic of the region (Wright & Zarza, 1990). Munsell color analysis showed differences between the samples (7.5 YR 4/3 in M8 and 10 YR 5/4 in M10), reflecting variations in oxidation, mineral content, and environmental conditions during deposition (Russell, 1889).

In terms of grain size, sorting ranged from moderately well sorted (σ_ϕ: 1.67 in M8) to poorly sorted (σ_ϕ: 1.83 in M10), indicating variability in flow intensity (Ducloux et al., 1998). Both samples displayed negative skewness (−0.25 in M8 and −0.55 in M10), suggesting a greater proportion of coarse particles, typical of high-energy environments (Al-Farraj & Harvey, 2000). Low kurtosis values (0.40 in M8 and 0.48 in M10) indicate a flat and uniform grain-size distribution, characteristic of consistent and turbulent flows (Greenbaum et al., 2020; Wanas et al., 2015; Glasby et al., 2010).

Table 4 – Sysgran analysis results for samples M8 and M10 – micro-watershed 3, Los Volcanes sector.

Site	Sample	UTM East	UTM South	Depth (M/Cm)	Initial Weight (g)	Final Weight (g)	Error %	Munsell Color	Sorting (Σ_Φ)	Skewness (A_Φ)	Kurtosis (K_Φ)
Downstream	M8	371354	6971524	92cm	1034,05	1031,05	0%	7.5 YR 4/3 (dark yellowish brown)	1.67	-0.25	0.40
Upstream	M10	371660	6971497	98cm	1035,76	1031,74	0%	10 YR 5/4 (moderate yellowish brown)	1.83	-0.55	0.48

Source: Authors (2024).

3.4 Micro-watershed 5 (Andacollo Sector)

Six sediment samples were collected from the central ravine of micro-watershed 5: downstream (M6: 49.61% gravel, 48.30% sand, 1.81% silt, 0.28% clay; M11: 55.40% gravel, 40.34% sand, 4.04% silt, 0.22% clay), midstream (M3: 61.18% gravel, 30.49% sand, 4.51% silt, 3.82% clay; M5: 51.09% gravel, 46.56% sand, 1.92% silt, 0.43% clay), and upstream (M1a: 53.82% gravel, 38.17% sand, 5.02% silt, 2.99% clay; M2b: 42.40% gravel, 41.89% sand, 7.57% silt, 8.14% clay). Samples were taken from alluvial-colluvial deposits, displaying a gravelly sand texture, schistose structure, and light plasticity.

Grain-size analysis revealed that sediments are predominantly composed of gravel and sand, with angular and loose particles. According to Moreno (2014), the concentration of fine sediments (<200 micrometers) was as follows: M6 (1.04%), M11 (2.13%), M3 (4.16%), M5 (1.17%), M1a (4%), and M2b (7.8%).

In the downstream samples (M6 and M11), the flow is turbulent, with high transport capacity for coarse particles (gravel: 49.61%–55.40%; sand: 40.34%–48.30%), indicating active depositional processes. In the midstream section (M3 and M5), gravel proportions are higher (61.18% in M3 and 51.09% in M5), while the higher fine sediment concentrations in M3 (8.33%) and M5 (2.35%) suggest lower-intensity events that allowed finer particles to settle. Upstream (M1a and M2b), the flow is characterized by relatively lower energy, with balanced proportions of gravel and sand (gravel: 42.40%–53.82%; sand: 38.17%–41.89%) and higher concentrations of fine sediments (5.02%–7.57%).

The grain-size and physical variability reflect a dynamic fluvial system influenced by episodic high-energy events. The shallowest deposits (1 m) are associated with recent events, whereas the deeper ones (up to 7 meters) represent older and more compacted processes. Variable weight loss among the samples (0%–6%) suggests differences in compaction and moisture content (Figure 10).

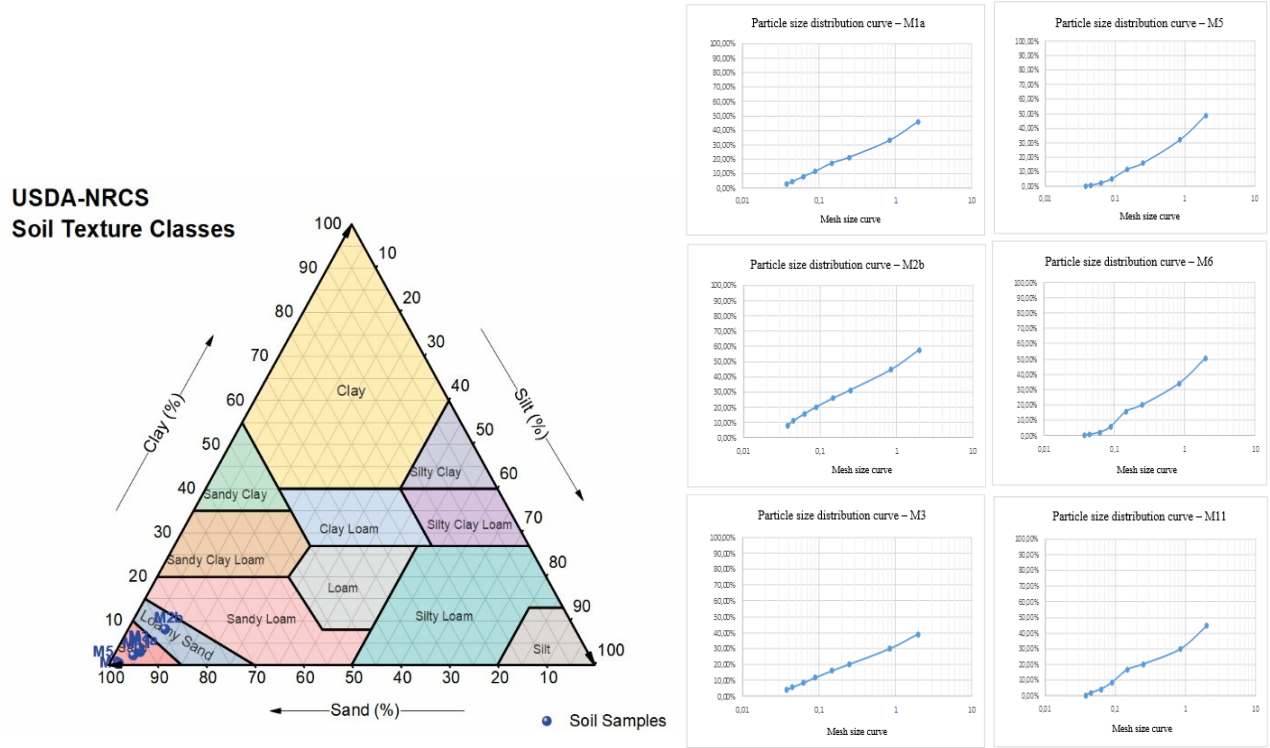

Figure 10 – Textural analysis results and grain-size distribution curves for samples M1a, M2b, M3, M5, M6, and M11 from micro-watershed 5, Andacollo sector.
Source: Authors (2024).

All samples exhibited variability in weight loss ranging from 0% to 6%, attributable to the natural compaction of sediments, mechanical wear during transport, and fluctuations in moisture at the time of sampling (Porat et al., 1997; Gerson et al., 1993). Sampling depths ranged from 1 to 7 meters, reflecting different levels of alluvial deposition, with shallower deposits being more recent and deeper ones older and more compacted. The uniform lithology indicates a

common sediment source, transported, and deposited by flows from the surrounding mountains (Eitel et al., 2001; Melton, 1965). Color analysis ranged from 10 YR 6/3 to 10 YR 5/4, suggesting moderate oxidation and the presence of iron minerals, indicative of similar oxidation conditions (Bourquin et al., 2009).

Grain-size properties showed sorting values ranging from moderately well sorted (σ_ϕ: 1.15) to poorly sorted (σ_ϕ: 2.00), reflecting episodic flows capable of transporting particles of varying sizes (Ridgway & DeCelles, 1993). Positive skewness (α_ϕ > 1) in most samples indicates a higher proportion of fine particles, typical of low-energy environments (Hooke, 1967). Low kurtosis (K_ϕ < 1) suggests a uniform grain-size distribution (Hetz et al., 2013; Antinao & McDonald, 2013).

Table 5 – Sysgran analysis results for samples M1a, M2b, M3, M5, M6, and M11 – micro-watershed 5, Andacollo sector.

Site	Sample	UTM East	UTM South	Depth (M/Cm)	Initial Weight (g)	Final Weight (g)	Error %	Munsell Color	Sorting (Σ_Φ)	Skewness (A_Φ)	Kurtosis (K_Φ)
Upstream	M1a	371345	6975894	4m	883,49	833,49	6%	10 YR 6/3 (light yellowish brown)	1,57	1,36	0,89
Upstream	M2b	370897	6974667	6m	835,11	804,91	4%	10 YR 6/3 (light yellowish brown)	2	0,83	0,74
Middle course	M3	370917	6974364	1m	836,5	796,27	5%	10 YR 5/3 (moderate yellowish brown)	1,53	1,32	1,04
Middle course	M5	370509	6973597	1m	908,15	857,82	6%	10 YR 5/4 (moderate yellowish brown)	1,15	1,51	0,81
Downstream	M6	370955	6974360	1m	937,7	887,52	5%	10 YR 5/3 (moderate yellowish brown)	1,4	1,41	0,74
Downstream	M11	370509	6973597	7m	1040	1039,6	0%	10 YR 5/4 (moderate yellowish brown)	1,45	1,38	0,84

Source: Authors (2024).

4. Conclusion

The analysis of micro-watersheds 1 (Borgoño sector), 2 (Cartavio sector), 3 (Los Volcanes sector), and 5 (Andacollo sector) within the Copiapó River basin reveals a sedimentary dynamic influenced by the arid climate, topography, and extreme hydrological events. The alluvial-fluvial system, characterized by transitional to turbulent flows, reflects local variations in flow energy that shape the landscape.

In micro-watershed 1 (Borgoño sector), coarse sand sediments rich in ferruginous nodules and marked by negative skewness indicate high-energy flows capable of transporting large particles. Lower slopes downstream favor the deposition of loose material in response to episodic events and geomorphological features.

Micro-watershed 2 (Cartavio sector) features gravel and sand deposits with low cohesion, resulting from mass-wasting events and landslides. Variations in skewness and kurtosis reflect a gradual decrease in flow energy along the ravine, with coarse particle deposition occurring in lower-slope areas typical of alluvial-colluvial systems.

In micro-watershed 3 (Los Volcanes sector), coarse sands, iron oxide staining, and poor grain-size sorting point to fluctuating and unstable flows. These are driven by seasonal variability and sudden rainfall events, which transport loose, non-cohesive particles and reshape the arid terrain.

Micro-watershed 5 (Andacollo sector) is characterized by abundant gravel and coarse sand transported by high-energy flows. Poor sorting and, in some cases, positive skewness suggest suspended fine particles. The depth of the deposits (1–7 m) reflects a complex sedimentary history, with multiple flow events mobilizing materials at various stratigraphic levels.

Overall, the micro-watersheds display low-cohesion sediments highly susceptible to erosion during intense rainfall. The presence of angular, non-cohesive particles—mainly gravels and sands—favors the initiation of debris flows on steep slopes, shaping a landscape with high erosion potential, typical of arid regions.

The dynamics of debris flows in this arid region play a critical role in landscape formation and represent significant geological hazards. Understanding these processes is essential for effective risk planning and management in Atacama, helping to mitigate natural disasters in areas vulnerable to erosion and sediment transport.

References

ANTONI, S. et al. Granulometric analysis of Lampuuk-Lhoknga Beach, Aceh Province. *IOP Conference Series: Earth and Environmental Science*, v. 348, n. 1, p. 012117, 2019. DOI: https://doi.org/10.1088/1755-1315/348/1/012117.

BIN, W. H.; MING, H. S. An improved mathematical model for geological analysis of debris flow. *Journal of Geography and Geology*, v. 6, n. 1, p. 129, 2014. DOI: https://doi.org/10.5539/jgg.v6n1p129.

BLASIO, F. V. D. *Non-Newtonian fluids, mudflows, and debris flows: a rheological approach*. Dordrecht: Springer, 2011. p. 89. DOI: https://doi.org/10.1007/978-94-007-1122-8_4.

CAMARGO, M. G. SysGran: um sistema de código aberto para análises granulométricas do sedimento. *Revista Brasileira de Geociências*, v. 36, n. 2, p. 371-378, 2006.

GONÇALVES, G. M. S. et al. Granulometria do sedimento de fundo do canal São Gonçalo na região do Porto de Pelotas. *Revista Ambientale*, v. 13, n. 2, p. 60, 2021. DOI: https://doi.org/10.48180/ambientale.v13i2.296.

GONZÁLEZ, A.; MATTAR, C.; SEPÚLVEDA, H. H. Análisis de los forzantes climáticos y antropogénicos en la reducción de agua en la cuenca del río Copiapó, Chile (28° S) utilizando productos satelitales. *Revista de Teledetección*, n. 63, p. 53-63, 2024. DOI: https://doi.org/10.4995/raet.2024.20047.

GUTIÉRREZ, J. P. et al. Natural recovery of infiltration capacity in simulated bank filtration of highly turbid waters. *Water Research*, v. 147, p. 299, 2018. DOI: https://doi.org/10.1016/j.watres.2018.10.009.

HAAS, T. de; WOERKOM, T. van. Bed scour by debris flows: experimental investigation of effects of debris-flow composition. *Earth Surface Processes and Landforms*, v. 41, n. 13, p. 1951, 2016. DOI: https://doi.org/10.1002/esp.3963.

HU, W. et al. Sensitivity of the initiation and runout of flowslides in loose granular deposits to the content of small particles: an insight from flume tests. *Engineering Geology*, v. 231, p. 34, 2017. DOI: https://doi.org/10.1016/j.enggeo.2017.10.001.

HÜRLIMANN, M. et al. Debris-flow monitoring and warning: review and examples. *Earth-Science Reviews*, v. 199, p. 102981, 2019. DOI: https://doi.org/10.1016/j.earscirev.2019.102981.

IVERSON, R. M.; GEORGE, D. L. A depth-averaged debris-flow model that includes the effects of evolving dilatancy. *Proceedings of the Royal Society A*, 2023. DOI: https://royalsocietypublishing.org/doi/10.1098/rspa.2013.0819.

IZQUIERDO, T. et al. Historical catastrophic floods at the southern edge of the Atacama Desert: a multi-archive reconstruction of the Copiapó river extreme events. *Global and Planetary Change*, v. 236, p. 104411, 2024. DOI: https://doi.org/10.1016/j.gloplacha.2024.104411.

JAAPAR, A. R. et al. The emerging widespread debris flow disasters in tropical terrain of Peninsular Malaysia: understanding the risk and policy intervention. *E3S Web of Conferences*, v. 415, p. 5008, 2023. DOI: https://doi.org/10.1051/e3sconf/202341505008.

LLORENTE, V. J.; PADILLA, E. M.; DÍEZ-MINGUITO, M. Non-newtonian wind-driven flows in homogeneous semienclosed basins. *arXiv* (Cornell University), 2023. DOI: https://doi.org/10.48550/arxiv.2306.07624.

LÓPEZ, J. C.; TOLEDO, M. Á.; MOYA, R. M. A unified view of nonlinear resistance formulas for seepage flow in coarse granular media. *Water*, v. 13, n. 14, p. 1967, 2021. DOI: https://doi.org/10.3390/w13141967.

OUYANG, C. et al. An example of a hazard and risk assessment for debris flows: a case study of Niwan Gully, Wudu, China. *Engineering Geology*, v. 263, p. 105351, 2019. DOI: https://doi.org/10.1016/j.enggeo.2019.105351.

PELLEGRINO, A.; SCHIPPA, L. Rheological modeling of macro viscous flows of granular suspension of regular and irregular particles. *Water*, v. 10, n. 1, p. 21, 2017. DOI: https://doi.org/10.3390/w10010021.

PRANOTO, W. A.; SUBARI, M. Study of sediment transport discharges of Citarum River, West Java in laboratory. *IOP Conference Series: Materials Science and Engineering*, v. 650, n. 1, p. 012059, 2019. DOI: https://doi.org/10.1088/1757-899X/650/1/012059.

SIVAK, E.; VOLKOVA, S. N. Transformation of land resources as a result of anthropogenic impact. *E3S Web of Conferences*, v. 175, p. 6002, 2020. DOI: https://doi.org/10.1051/e3sconf/202017506002.

WU, H.; HE, N.; ZHANG, X. Numerical model of viscous debris flows with depth-dependent yield strength. *Journal of GeoEngineering*, v. 10, n. 1, p. 1, 2015. DOI: https://doi.org/10.6310/jog.2015.10(1).1.

WU, X. et al. Discontinuity in equilibrium wave-current ripple size and shape caused by a winnowing threshold in cohesive sand-clay beds. *Earth and Space Science Open Archive*, 2021. DOI: https://doi.org/10.1002/essoar.10508217.1.

ZAINOL, M. R. R. M. A.; AWAHAB, M. K. Hydraulic physical model of debris flow for Malaysia case study. *IOP Conference Series: Materials Science and Engineering*, v. 374, p. 012067, 2018. DOI: https://doi.org/10.1088/1757-899X/374/1/012067.